Timo Tigges*, Jonas Rockstroh, Alexandru Pielmuş, Michael Klum, Aarne Feldheiser, Oliver Hunsicker and Reinhold Orglmeister

In-ear photoplethysmography for central pulse waveform analysis in non-invasive hemodynamic monitoring

Abstract: In recent years, the analysis of the photoplethys-mographic (PPG) pulse waveforms has attracted much research focus. However, the considered signals are primarily recorded at the fingertips, which suffer from reduced peripheral perfusion in situations like hypovolemia or sepsis, rendering waveform analysis infeasible. The ear canal is not affected by cardiovascular centralization and could thus prove to be an ideal alternate measurement site for pulse waveform analysis. Therefore, we developed a novel system that allows for highly accurate photoplethysmographic measurements in the ear canal. We conducted a measurement study in order to assess the signal-to-noise ratio of our developed system Hereby, we achieved a mean SNR of 40.65 dB. Hence, we could show that our system allows for highly accurate PPG recordings in the ear canal facilitating sophisticated pulse waveform analysis. Furthermore, we demonstrated that the pulse decomposition analysis is also applicable to in-ear PPG recordings.

1 Introduction

In recent years, the analysis of the photoplethysmographic (PPG) pulse waveforms has attracted much research focus. However, the considered signals are primarily recorded at the fingertips, which suffer from reduced peripheral perfusion in situations like hypovolemia or sepsis, rendering waveform

analysis infeasible. The ear canal is not affected by cardiovascular centralisation and is thus a promising alternate measurement site for pulse waveform analysis. Therefore, we developed a novel system that allows for highly accurate photoplethysmographic measurements in the ear canal.

For the extraction of physiologically relevant information from single volume pulse cycles, the pulse decomposition analysis (PDA) has proven to be a powerful tool [1]. In the PDA, a single volume cycle is modelled as a linear superposition of basis functions. In this work, we show for the first time, that the PDA can also be applied to photoplethysmographic signals that are recorded from within the ear canal.

This paper is organized as follows: In Section 2, firstly, the develop in-ear PPG sensor system is presented. Next, the conducted approach to signal quality assessment is outlined. Then, the proposed PDA model is described. Section 3 contains the results of the signal quality assessment and shows that the PDA is applicable to in-ear PPG recordings. Finally, concluding remarks are given in Section 4.

2 Methods

2.1 In-ear-PPG sensor concept

We developed a novel in-ear-PPG sensor that consists of three main parts, an optical sensor that can be introduced into the ear canal, an analog front-end that handles signal
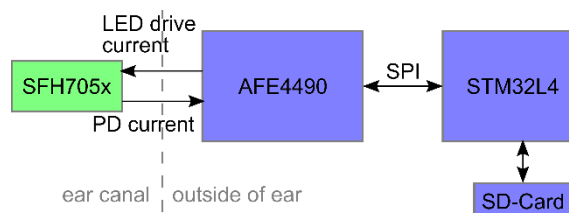
──────

*Corresponding author: Timo Tigges: Chair of Electronics and Medical Signal Processing, Technische Universität Berlin, Berlin, Germany, e-mail: timo.tigges@tu-berlin.de
Jonas Rockstroh, Alexandru Pielmuş, Michael Klum, Reinhold Orglmeister: Chair of Electronics and Medical Signal Processing, Technische Universität Berlin, Berlin, Germany
Aarne Feldheiser, Oliver Hunsicker: Department of Anaesthesiology and Intensive Care Medicine, Campus Virchow-Klinikum, Charité - University Medicine Berlin, Germany, e-mail: aarne.feldheiser@charite.de

Figure 1: Sensor concept

Figure 2 a) In-ear PPG system prototype attached to the head. b) Axially oriented optical sensor with off-the-shelf foam earbud adapter. c) Radially oriented optical sensor with off-the-shelf rubber earbud adapter**.**

conditioning and analog-to-digital conversion and a low-power microcontroller. A block diagram that describes the system is depicted in **Figure 1**.

The optical sensor is based on an OSRAM SFH 7051, an integrated combination of three green light emitting diodes with a peak emission wavelength of 530 nm and a matching photodetector. The sensor package measures only 4.7 mm x 2.5 mm x 0.9 mm and is thus small enough to be placed within the outer ear canal (the tragus). The optical sensor can be placed in disposable, off-the-shelf foam or rubber earbud adapters of different sizing, which allows for easy per-patient customization and facilitates sanitation. We constructed sensors both with axial and radial alignment with respect to the ear canal. Two prototype sensors are presented in **Figure 2**.

We connected the optical sensor to an integrated analog front-end, a Texas Instruments AFE 4490, which is an integrated circuit that is specifically designed for photoplethysmographic measurements. The AFE 4490 incorporates a LED driver with 8-Bit current resolution and a configurable three-stage receive channel that performs analog signal conditioning by consecutive transimpedance amplification, DC offest cancellation and AC signal amplification and optional filtering. All three stages can be manually tuned. For subsequent analog-to-digital conversion, a 22-Bit ADC is also integrated.

Next, the integrated front-end was interfaced with a STM32L476, an ultra-low-power microcontroller from STMicroelectronics with an ARM Cortex-M4 core. The communication between the AFE 4490 and the microcontroller was established by an SPI interface clocked at 8 MHz. All measurement data and logged events were stored on a micro-SD card. Furthermore, an automated calibration scheme was implemented on the microcontroller

that gradually adapts the analog signal conditioning for achieving a maximum pulse amplitude.

2.2 Signal quality assessment by SNR estimation

For assessing the signal quality of the developed system, we conducted a small measurement study comprised of eight healthy volunteers, aged 23 to 56 years. We recorded measurements of at least 60 s for both the optical sensor with radial and axial alignment per volunteer. During the measurements, the volunteers remained seated. As earbud adapters, the rubber version was used, whereby the volunteers could freely choose from different adapter sizes. Following a brief instruction, the volunteers themselves conducted the positioning of the respective sensor into the ear canal.

As an index for the signal quality, we calculated the signal-to-noise ratio (SNR) as defined by the equation

$$SNR = 10 \, log_{10} \left(\frac{\sum_{f_k=f_{sig,low}}^{f_{sig,high}} PSD(f_k)}{\sum_{f_k=f_{sig,high}}^{f_{Ny}} PSD(f_k)} \right), \qquad (1)$$

where $PSD(f_k)$ denotes the power spectral density estimate in frequency bin f_k, $f_{sig,low}$ and $f_{sig,high}$ are the lower and upper frequency limit of the pulse signal and f_{Ny} is the maximum frequency component in the time discrete pulse signal, i.e. the Nyquist rate. The power spectral density was estimated by Welch's method. The sampling rate was set to 500 samples/second during all measurements (i.e. $f_{Ny} = 250$). No digital filtering was performed prior to the SNR calculations.

2.3 Pulse waveform analysis by decomposition into basis functions

In the pulse decomposition analysis, a single pulse is modelled as a linear superposition of basis functions where each basis function is meant to represent a pressure wave of different origin from within the cardiovascular system, e.g. a wave reflection at a major arterial junction. The variable parameters in the PDA model can be found by solving a least-squares parameter optimization problem.

In this work, we utilize the basis function $g(t, \boldsymbol{\theta})$, which is based on the well-known Gamma distribution, as defined by the equation

$$g(t, \boldsymbol{\theta}) = \frac{\beta^\alpha}{s\Gamma(\alpha)} t^{\alpha-1} e^{-\beta t}, \qquad (2)$$

where t represents the time, the function parameters α, β and s determine the shape, location and amplitude of the basis function and Γ denotes the Gamma function. For the sake of easier interpretation and in order to facilitate the formulation of meaningful boundary conditions for the optimization problem, we derive the basis function parameters from the amplitude b, the mode m (i.e. the location of the maximum) and the variance σ (i.e. the width) of the basis function as given by the set of equations:

$$\alpha = \frac{1}{2\sigma}\left(m^2 + m\sqrt{m^2 + 4\sigma}\right) + 2, \qquad (2)$$

$$\beta = \frac{1}{2\sigma}\left(m + \sqrt{m^2 + 4\sigma}\right), \qquad (2)$$

$$\text{and } s = \frac{1}{b}\frac{\beta^\alpha}{\Gamma(\alpha)}\left(\frac{\alpha-1}{\beta}\right)^{\alpha-1} e^{(1-\alpha)}. \qquad (2)$$

The vector of tunable parameters can thus conveniently be formulated as $\boldsymbol{\theta} = (b, m, \sigma)$.

Next, we modelled a single volume pulse as a superposition of three pulse waves. Thus, the PDA model was defined by the following equation:

$$\begin{aligned} y(t) &= f(t, \boldsymbol{\theta}) + \varepsilon(t) \\ &= \sum_{m=1}^{3} g_m(t, \boldsymbol{\theta_m}) + \varepsilon(t), \end{aligned} \qquad (6)$$

where $y(t)$ represents a single volume pulse (i.e. the target variable) and $\varepsilon(t)$ is the model residual. For a comprehensive description of the PDA model as well as for our approach to the PDA model selection problem, the reader is kindly referred to [4]. From a physiological viewpoint, the first wave could be regarded as originating directly from the ventricular contraction. The second pulse is thought of being a reflection at the junction between the thoracic and abdominal aorta, as there is a significant decrease in the artery diameter. Similarly, the change in diameter at the juncture between the abdominal aorta and the iliac arteries is regarded to be responsible for the third pulse wave [1]

In order to find the unknown model parameters $\boldsymbol{\theta}$ we needed to solve the following optimization problem:

$$\min_{\theta} \sum_{n=1}^{N}[f(t_n, \boldsymbol{\theta}) - y(t_n)]^2 \qquad (7)$$
$$\text{subject to } h(\boldsymbol{\theta}) \leq 0 \text{ and } lb \leq \boldsymbol{\theta} \leq ub,$$

where $h(\boldsymbol{\theta})$, lb and ub are the linear constraints and the upper and lower boundaries within the solution space. For a robust solution to the described problem, an interior pont algorithm was employed. **Figure 3** shows the pulse decomposition of an example volume pulse that was recorded from within the ear canal by our developed sensor system conducted with the proposed algorithm.
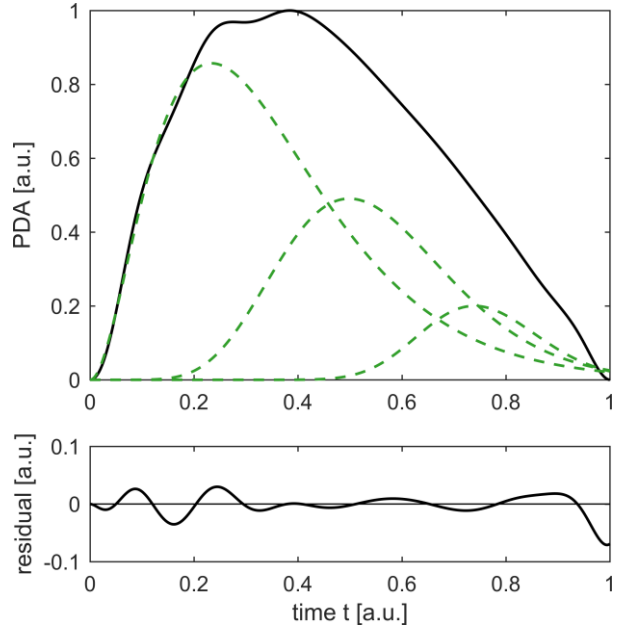

Figure3: Pulse Decomposition analysis applied to an example in-ear PPG pulse

3 Results

3.1 Signal quality assessment

From the recordings of our conducted measurement study, we were able to estimate the SNR values for both the radially and axially oriented optical sensor. SNR calculations were performed in accordance with the description given in Section 2.2. Analogously to previous studies [2], a lower limit of 0.5 Hz was chosen for the useful PPG signal bandwidth. With respect to the upper limit, we performed SNR calculations for two different threshold values. Firstly, the upper limit was set to be 10 Hz, as it was previously described by Venema, et al. [2]. We believe this limit does exclude a significant frequential component of the PPG signal bandwidth. Therefore, secondly, we also performed SNR calculations with an upper limit of 20 Hz, which is more conforming to cut-off frequencies of low-pass filters that were employed in previous PDA studies [5].

For the axially oriented sensor, we estimated a mean SNR value of 23.0 dB for an upper limit of 10 Hz. The estimated mean SNR value for an upper limit of 20 Hz was 24.2 dB. This increase is easily explainable by the bigger bandwidth that is attributed to the useful PPG signal. A detailed listing of the SNR assessment results for the axially oriented sensor can be found in **Table 2**.

Table 2: In-ear PPG signal quality estimated by SNR values (Min – minimum, Max – maximum, STD – standard deviation) for the axial sensor orientation (given in dB).

	Min	Max	Mean	STD
SNR (0.5 Hz - 10 Hz)	11.3	32.5	**23.0**	7.0
SNR (0.5 Hz - 20 Hz)	11.3	36.8	**24.2**	8.4

The use of the radially oriented optical sensor resulted in significantly better results, as we calculated mean SNR values of 33.9 dB and 40.7 dB for the upper PPG bandwidth limits of 10 Hz and 20 Hz, respectively. A summary of the estimated SNR values for the radial sensor is listed in table **Table 3**.

Table 3: In-ear PPG signal quality estimated by SNR values (Min – minimum, Max – maximum, STD – standard deviation) for the radial sensor orientation (given in dB).

	Min	Max	Mean	STD
SNR (0.5 Hz - 10 Hz)	28.5	40.7	**33.9**	3.6
SNR (0.5 Hz - 20 Hz)	32.7	49.3	**40.7**	6.0

This signal quality difference is attributed to the fact that the optical coupling of the radial sensor into the tissue in the ear canal is better. Consequently, the proportion of light reaching the photodetector that is modulated by the pulsating blood volume is bigger.

An example signal recorded with the radially oriented optical sensor is given in **Figure 4**. The top graph shows the original signal which was not digitally processed. The bottom graph shows the same signal interval after applying a zero-phase bandpass filter with cut-off frequencies of 0.5 Hz and 20 Hz. Furthermore, the pulse decomposition analysis outcome is also shown.
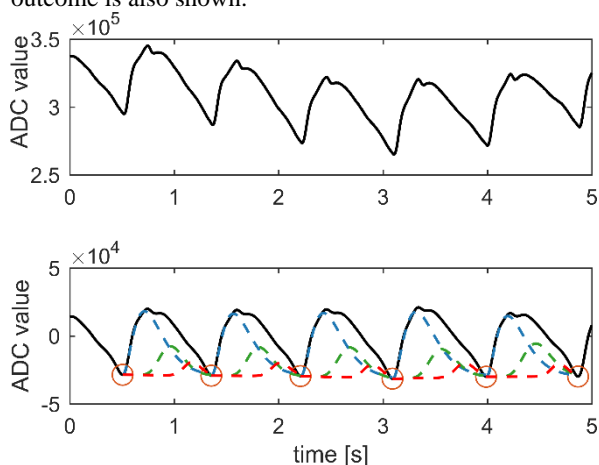

Figure 4: An example in-ear PPG signal recorded with the radially oriented sensor. The top graph shows the unfiltered raw signal. The bottom graph

4 Conclusion

We could show that our system allows for highly accurate PPG recordings in the ear canal facilitating sophisticated pulse waveform analysis.

References

[1] M. C. Baruch, D. E. Warburton, S. S. Bredin, A. Cote, D. W. Gerdt and C. M. Adkins, "Pulse decomposition analysis of the digital arterial pulse during hemorrhage simulation." Nonlinear biomedical physics, vol. 5, p. 1, Jan. 2011

[2] B. Venema u. a. „Advances in Refl ective Oxygen Saturation Monitoring with a Novel In-Ear Sensor System: Results of a Human Hypoxia Study". In: IEEE Transactions on Biomedical Engineering 59.7 (Juli 2012) S. 2003–2010. doi: 10.1109/tbme.2012.2196276

[3] W. Zong, T. Heldt, G. Moody, and R. Mark, "An open-source algorithm to detect onset of arterial blood pressure pulses," in Computers in Cardiology, 2003, Sept. 2003, pp. 259–262.

[4] T. Tigges, A. Pielmuş, M. Klum, A. Feldheiser, O. Hunsicker, R. Orglmeister, „Model Selection for the Pulse Decomposition Analysis of Fingertip Photoplethysmograms", submitted to 39th Annual International Conference of the IEEE Engineering in Medicine and Biology Society.

[5] R. Couceiro, P. Carvalho, R. P. Paiva, J. Henriques, I. Quintal, M. Antunes, J. Muehlsteff, C. Eickholt, C. Brinkmeyer, M. Kelm, and C. Meyer, "Assessment of cardiovascular function from multi-gaussian fitting of a finger photoplethysmogram," Physiological Measurement, vol. 36, no. 9, p. 1801, 2015